Minimum Local Emissivity Variance Retrieval of Cloud Altitude and Effective Spectral Emissivity—Simulation and Initial Verification

HUNG-LUNG HUANG

Cooperative Institute for Meteorological Satellite Studies, University of Wisconsin—Madison, Madison, Wisconsin

WILLIAM L. SMITH

NASA Langley Research Center, Hampton, Virginia

JUN LI AND PAOLO ANTONELLI

Cooperative Institute for Meteorological Satellite Studies, University of Wisconsin—Madison, Madison, Wisconsin

XIANGQIAN WU

NOAA/NESDIS/Office of Research and Applications, Camp Springs, Maryland

ROBERT O. KNUTESON, BORMIN HUANG, AND BRIAN J. OSBORNE

Cooperative Institute for Meteorological Satellite Studies, University of Wisconsin—Madison, Madison, Wisconsin

(Manuscript received 17 July 2002, in final form 7 November 2003)

ABSTRACT

This paper describes the theory and application of the minimum local emissivity variance (MLEV) technique for simultaneous retrieval of cloud pressure level and effective spectral emissivity from high-spectral-resolution radiances, for the case of single-layer clouds. This technique, which has become feasible only with the recent development of high-spectral-resolution satellite and airborne instruments, is shown to provide reliable cloud spectral emissivity and pressure level under a wide range of atmospheric conditions. The MLEV algorithm uses a physical approach in which the local variances of spectral cloud emissivity are calculated for a number of assumed or first-guess cloud pressure levels. The optimal solution for the single-layer cloud emissivity spectrum is that having the ''minimum local emissivity variance'' among the retrieved emissivity spectra associated with different first-guess cloud pressure levels. This is due to the fact that the absorption, reflection, and scattering processes of clouds exhibit relatively limited localized spectral emissivity structure in the infrared 10–15-μm longwave region. In this simulation study it is shown that the MLEV cloud pressure root-mean-square errors for a single level with effective cloud emissivity greater than 0.1 are ~30, ~10, and ~50 hPa, for high (200–300 hPa), middle (500 hPa), and low (850 hPa) clouds, respectively. The associated cloud emissivity root-mean-square errors in the 900 cm^{-1} spectral channel are less than 0.05, 0.04, and 0.25 for high, middle, and low clouds, respectively.

1. Introduction

New instruments such as the Atmospheric Infrared Sounder, Interferometric Monitor for Greenhouse Gases, Geosynchronous Imaging Fourier Transform Spectrometer (GIFTS), Cross-Track Infrared Sounder, Infrared Atmospheric Sounding Interferometer, the Hyperspectral Environmental Suite on Geostationary Operational Environmental Satellite (GOES)-R, and others provide researchers with the potential to make significant advancements in cloud property retrieval. This is a result not only of their high spectral resolution, but also their relatively broad spectral coverage.

Although a number of techniques, such as the carbon dioxide (CO_2) slicing technique (Smith and Platt 1978; Menzel et al. 1983), minimum residual method (Eyre and Menzel 1989), and, more recent, the variational approach (Li et al. 2001) have been developed for retrieving effective cloud emissivity (a product of spectrally dependent cloud emissivity and cloud-cover fraction) and effective cloud-top pressure, they provide the emissivity for only a single wavenumber and are known

Corresponding author address: Dr. H.-L. Allen Huang, Cooperative Institute for Meteorological Satellite Studies, University of Wisconsin—Madison, 1225 West Dayton Street, Madison, WI 53706.
E-mail: allenh@ssec.wisc.edu

to work for only single-layer, semigray (nonblack) mid- to high-level clouds.

In this paper, we describe a technique for the simultaneous retrieval of the cloud pressure level and effective emissivity *spectrum* that takes advantage of the high-spectral-resolution radiances available with the types of instruments listed above, with samples taken throughout large portions of the infrared spectrum at a spectral resolution of 0.25–1 cm^{-1}.

In section 2, we give a detailed derivation of the minimum local emissivity variance (MLEV) algorithm. Sensitivity functions are derived analytically and are used to investigate the expected emissivity and cloud pressure level information content of the observed radiances for a number of model atmospheres. In section 3, the algorithm's performance is assessed using synthetic GIFTS data (Huang et al. 2000) in an attempt to evaluate the suitability of MLEV as a retrieval technique for real GIFTS-like hyperspectral data. Section 4 describes a preliminary case study involving the application of MLEV to measured radiances from the High-Resolution Interferometer Sounder (HIS; Smith et al. 1993) obtained during the Subsonic Aircraft Contrail and Cloud Effects Special Study (SUCCESS) field program (Toon and Miake-Lye 1998). In section 5, we discuss the overall performance of the technique, its limitations, and anticipated future work.

2. Theory

a. Algorithm derivation

If scattering processes, which are negligible in the spectral region used in the MLEV algorithm, are disregarded, the infrared clear-sky radiance measured by a high-spectral-resolution instrument for a specific spectral channel ν within an instantaneous field of view (IFOV) (Huang et al. 2002) is

$$R_{\mathrm{clr},\nu} = \varepsilon_{s,\nu} B_{s,\nu} \tau_{s,\nu} + \int_{\tau_{P_s}}^{\tau_0} B_\nu \, d\tau_\nu + (1 - \varepsilon_{s,\nu}) \int_{\tau_0}^{\tau_{P_s}} B_\nu \, d\tau_\nu^*. \quad (1)$$

Here, $\varepsilon_{s,\nu}$ is the surface emissivity, subscripts s and ν denote the surface and wavenumber, respectively, B is the Planck radiance, τ_{P_s} and τ_0 are the upward transmittance to the top of the atmosphere at surface pressure P_s and 0 hPa, respectively, and $\tau^* = \tau_s^2/\tau$ is a variable related to the downward transmittance. For a completely cloud-covered IFOV with an opaque cloud ($\varepsilon_c = 1$) at pressure P_c, the observed radiance is

$$R_{\mathrm{cld},\nu} = B_{c,\nu} \tau_{c,\nu} + \int_{\tau_{P_c}}^{\tau_0} B_\nu \, d\tau_\nu. \quad (2)$$

The upwelling radiance for a partially cloud-covered IFOV can then be written as a linear combination of clear and cloudy radiance terms:

$$R_\nu = (1 - N\varepsilon_{c,\nu}) R_{\mathrm{clr},\nu} + N\varepsilon_{c,\nu} R_{\mathrm{cld},\nu}, \quad (3)$$

where $N\varepsilon_{c,\nu}$ is the *effective cloud emissivity,* a product of the cloud emissivity $\varepsilon_{c,\nu}$ and the cloud fractional coverage N.

Recasting Eq. (3) in terms of the effective cloud emissivity, we obtain

$$N\varepsilon_{c,\nu} = \frac{R_\nu - R_{\mathrm{clr},\nu}}{R_{\mathrm{cld},\nu} - R_{\mathrm{clr},\nu}}, \quad (4)$$

which is the key relationship used in the application of the MLEV algorithm. In addition to the observed radiance R_ν, the algorithm requires an estimation of $R_{\mathrm{clr},\nu}$ and a calculation of $R_{\mathrm{cld},\nu}$ for each first-guess P_c. The fundamental principle of MLEV is to identify the P_c, out of all possible cloud levels from near the surface to 100 hPa, that minimizes the local emissivity variation (LEV) term

$$\mathrm{LEV}(P_c) = \sum_{\nu_1}^{\nu_2} (N\varepsilon_{c,\nu} - \overline{N\varepsilon_{c,\nu}})^2, \quad (5)$$

where

$$\overline{N\varepsilon_{c,\nu}} = \frac{\sum_{\nu-(\Delta\nu/2)}^{\nu+(\Delta\nu/2)} (N\varepsilon_{c,\nu})}{\Delta\nu}.$$

The cloud pressure level associated with the minimum of LEV (P_c) is the final solution. The optimal summation limits ν_1 and ν_2, with $\Delta\nu = \nu_1 - \nu_2 = 5$ cm^{-1} defining the local variance, were determined by sensitivity studies (described in detail below) and noise considerations to be 750 and 950 cm^{-1}, respectively.

If the assumed cloud pressure level is incorrect (under- or overestimated), $N\varepsilon_{c,\nu}$ will display a spectral structure correlated with water and carbon dioxide absorption lines, as we will demonstrate theoretically later. A correct cloud pressure level will result in a residual local variation that is due primarily to instrument noise, with the large-scale variation being due to the variation of emissivity associated with different types of clouds.

b. Sensitivity studies

In order to provide some theoretical insight into the expected performance of MLEV, let us first consider the sensitivity of the observed upwelling radiance to the effective cloud emissivity $N\varepsilon_{c,\nu}$ and to the cloud pressure level P_c for a range of atmospheric conditions and cloud pressure levels. It can be shown that the radiance sensitivity to $N\varepsilon_{c,\nu}$ and P_c can be given, respectively, by the magnitudes of the following derivatives (Li et al. 2001):

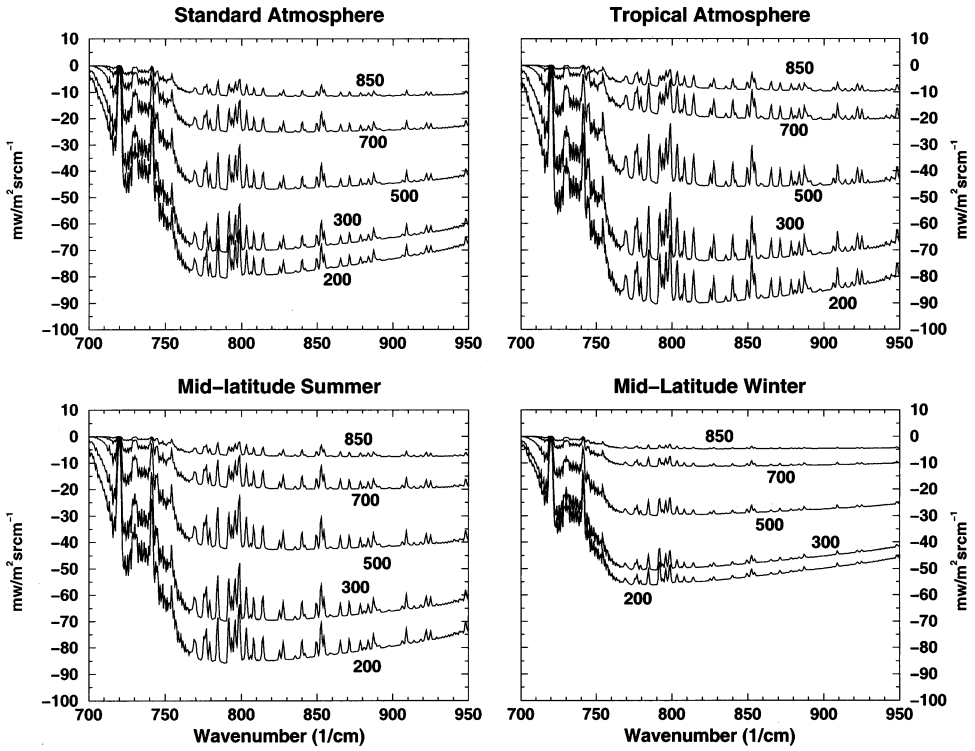

FIG. 1. Sensitivity functions for effective cloud emissivity spectrum, as defined by Eq. (6). The five cloud pressure levels are 200, 300, 500, 700, and 850 hPa, respectively.

$$\frac{\partial R_\nu}{\partial(N\varepsilon_{c,\nu})} = R_{\mathrm{cld},\nu} - R_{\mathrm{clr},\nu} \quad \text{and} \tag{6}$$

$$\frac{\partial R_\nu}{\partial P_c} = \frac{\partial B_{c,\nu}}{\partial P} N\varepsilon_{c,\nu}\tau_{P_c}. \tag{7}$$

Figures 1 and 2 show Eqs. (6) and (7), respectively, as determined for four model atmospheres (standard, tropical, midlatitude winter, and midlatitude summer; see Fig. 3) and five cloud pressure levels (200, 300, 500, 700, and 850 hPa) for an instrument with a spectral resolution of 0.625 cm^{-1}, similar to that of the GIFTS instrument in its high-resolution operating mode. High-latitude cases are excluded in this analysis, and therefore results are generally applicable primarily to geosynchronous platforms.

The spectral sensitivity function for effective emissivity [Eq. (6)] exhibits appreciable cloud pressure level and profile dependency (Fig. 1). Figure 1 illustrates that, for all model atmospheres considered, observed radiances will have the greatest sensitivity to $N\varepsilon_{c,\nu}$ for cloud at the 200-hPa level and the least sensitivity at 850 hPa. In spectral terms, radiances in the window channels have higher sensitivity than opaque channels. In particular, radiance observations in regions of strong CO_2 absorption are considerably less sensitive to $N\varepsilon_{c,\nu}$. Radiances in the 750–950 cm^{-1} region show the highest sensitivity to $N\varepsilon_{c,\nu}$; this consideration led to the choice of summation limits for Eq. (5) given earlier. The dependence of $N\varepsilon_{c,\nu}$ on the type of atmosphere can be seen most markedly in comparing the midlatitude summer and winter cases: a cold and near-isothermal atmosphere reduces the $N\varepsilon_{c,\nu}$ sensitivity of radiance measurements.

The radiance sensitivity to cloud pressure level [Eq. (7)] also exhibits significant model atmosphere dependence (Fig. 2). Note that the sensitivity to P_c is a function of both N and ε_c (for this analysis, the cloud fraction is assumed to be 1 and $\varepsilon_c = 0.95$). Radiances, therefore, have more sensitivity to opaque clouds than to transparent clouds and greater sensitivity in complete overcast than in scattered cloud conditions. Moreover, for the standard-atmosphere case near 200 hPa, $\partial B_{c,\nu}/\partial P$ is very small (locally isothermal; see Fig. 3) and results in a very limited sensitivity to P_c. In converse, for the tropical model atmosphere, the sensitivity to P_c at the 200-hPa cloud level is comparable to that of clouds at lower altitudes. Among the four cases (except for that of the 200-hPa cloud at standard atmosphere), radiances using the midlatitude winter model atmosphere have the least sensitivity to P_c because of smaller lapse rates and the reduced Planck function sensitivity at low temperatures. For the tropical case, the sensitivity to cloud pressure level for 200-hPa cloud matches that for lower-altitude clouds because of the more consistent lapse rates over different altitudes, suggesting that the most accurate cloud height retrievals obtained with MLEV will be under tropical conditions. As in the cloud emissivity

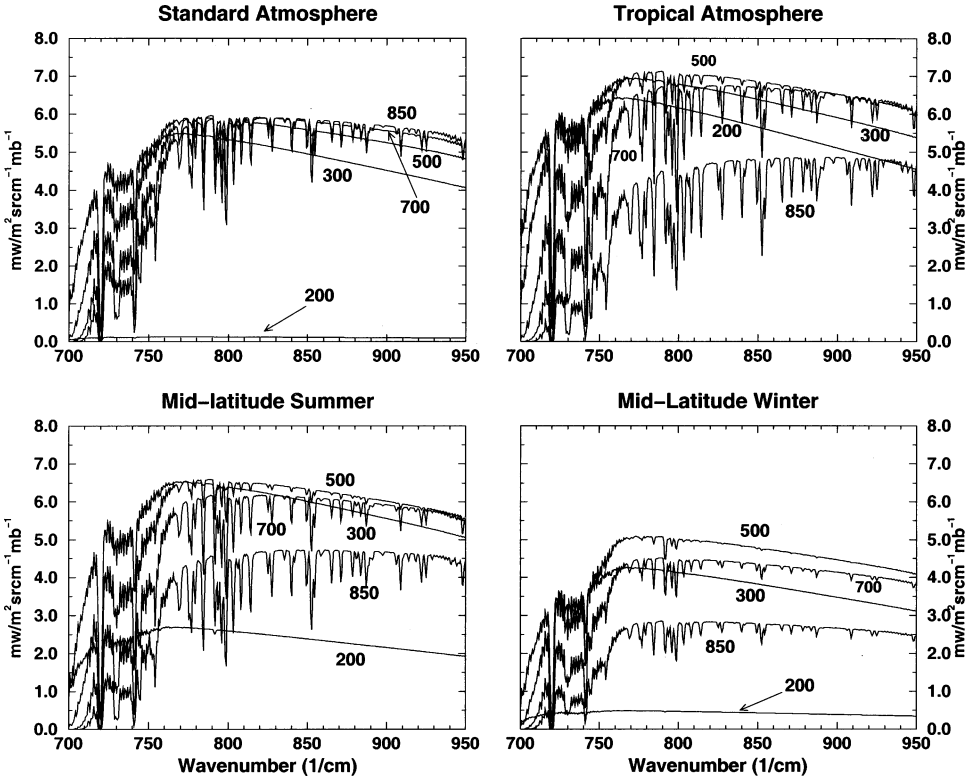

FIG. 2. Sensitivity functions for cloud pressure level, as defined by Eq. (7). The five cloud pressure levels are 200, 300, 500, 700, and 850 hPa, respectively.

case, the figures indicate that the 750–950 cm^{-1} region provides the greatest sensitivity to pressure level.

In summary, the sensitivity analysis described above indicates that low temperatures and vertically isothermal conditions will present MLEV with the most challenging conditions under which to retrieve spectral emissivity and cloud-level pressure. However, optimization of the cloud signal (at least cloud detection) can be explored through MLEV under these conditions, because $N\varepsilon_{c,\nu}$ and P_c can still provide complementary cloud sensitivities. For example, for the standard-atmosphere case, there is very little radiance sensitivity to cloud height for a 200-hPa cloud because it is locally isothermal, but cloud emissivity information is greater at this height.

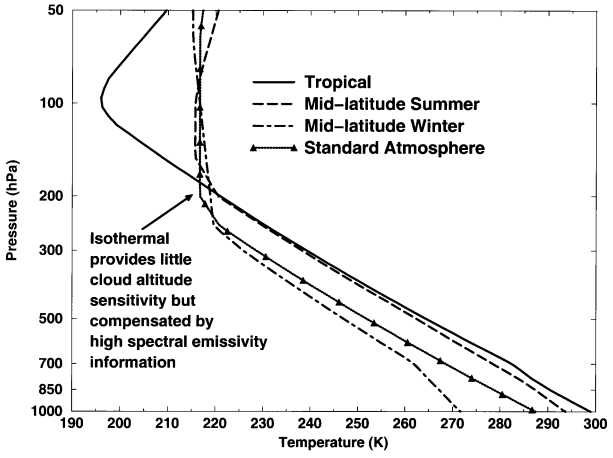

FIG. 3. Temperature profiles for the four model atmospheres used in MLEV simulations throughout this paper.

Let us now consider the sensitivity of the MLEV-derived effective cloud emissivity to incorrect estimates of $P_{c,}$ to demonstrate the primary foundation of MLEV—that an over- or underestimation of the cloud pressure level in Eq. (4) will result in an $N\varepsilon_{c,\nu}$ spectrum that, instead of being relatively smooth, exhibits a structure correlated with water and carbon dioxide absorption lines.

We start by looking at the effect of an inaccurate value of P_c on the observed radiances. If P_c is either overestimated (cloud level assumed to be too low) or underestimated (cloud level assumed to be too high), then the incorrect $R_{\mathrm{cld},\nu}$ can then be expressed as

$$R_{\mathrm{cld,over},\nu} = R_{\mathrm{cld},\nu} - \Delta R^{o}_{\nu} \quad \text{or} \tag{8}$$

$$R_{\mathrm{cld,under},\nu} = R_{\mathrm{cld},\nu} + \Delta R^{u}_{\nu}, \tag{9}$$

where the radiance residuals ΔR^{o}_{ν} and ΔR^{u}_{ν} are

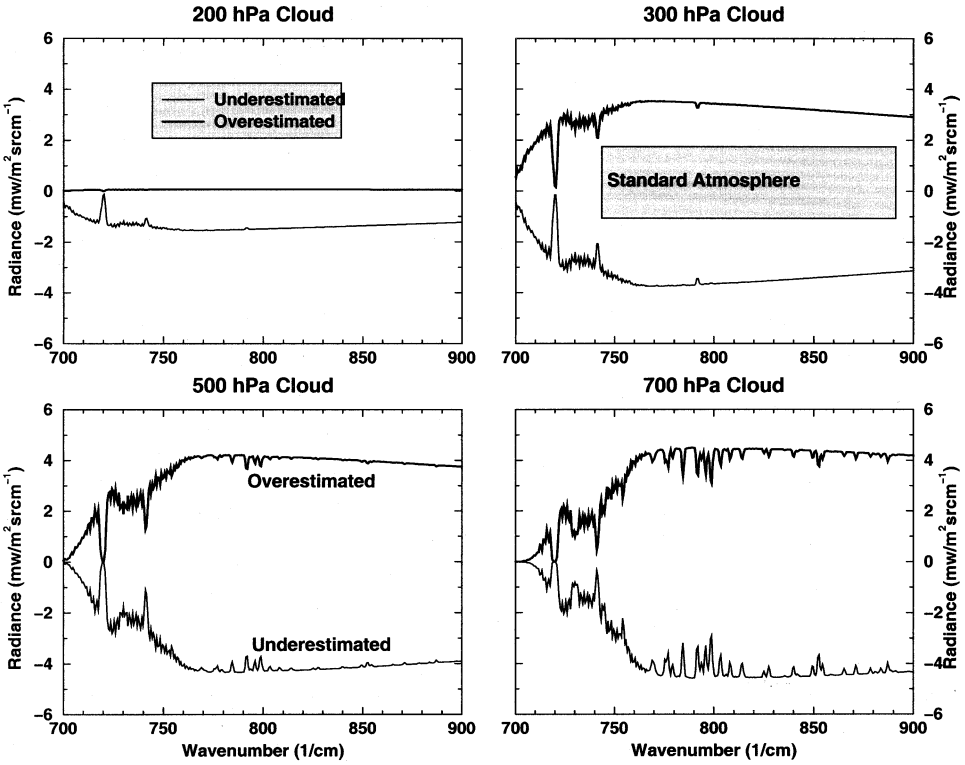

FIG. 4. The ΔR_ν^o for four different cloud levels, standard atmosphere [see Eq. (9)].

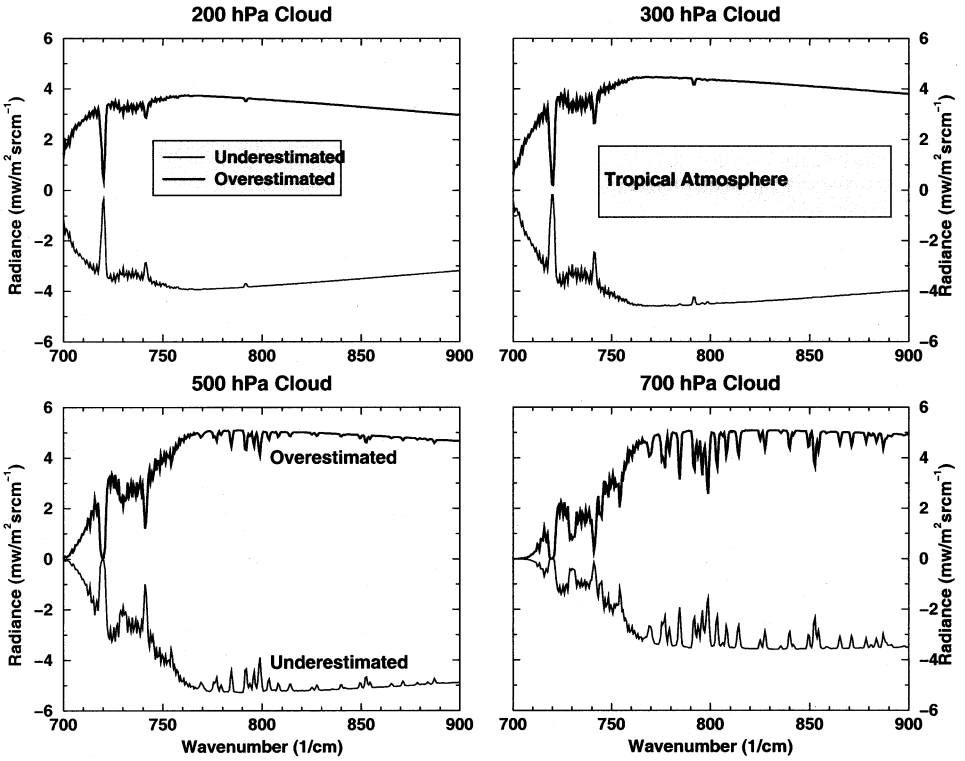

FIG. 5. The ΔR_ν^u for four different cloud levels, tropical atmosphere [see Eq. (10)].

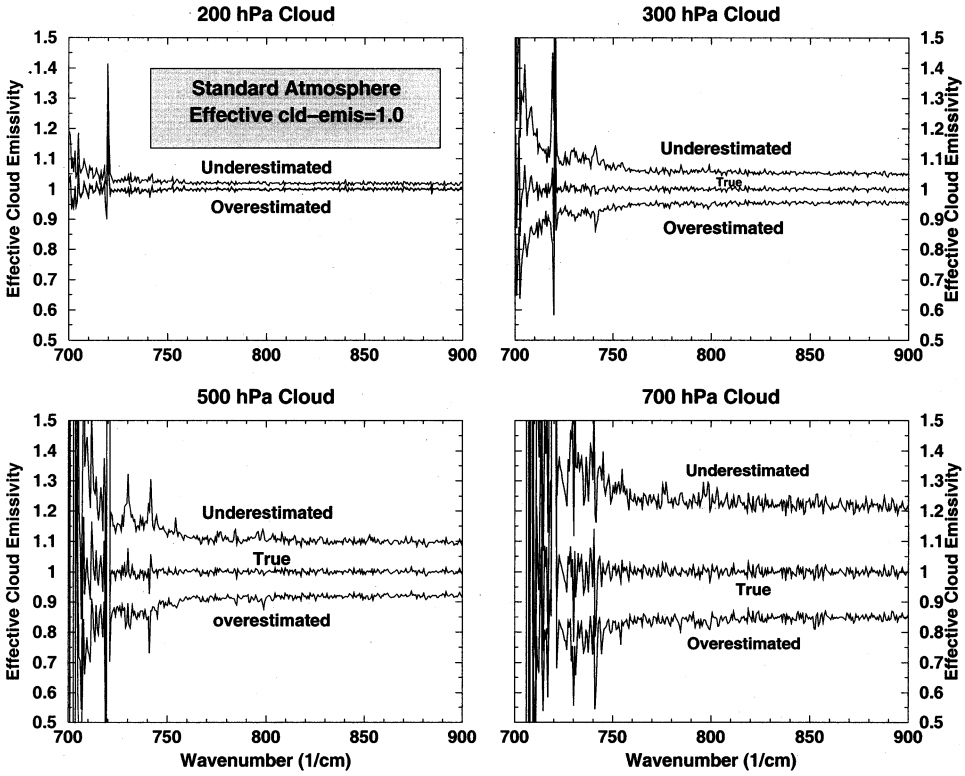

FIG. 6. Simulated MLEV-retrieved values of $N\varepsilon_{c,\nu}$, $N\varepsilon_{c,\nu,\text{over}}$, and $N\varepsilon_{c,\nu,\text{under}}$ for four different cloud levels, standard atmosphere, for a true value of $N\varepsilon_{c,\nu} = 1$.

$$\Delta R_\nu^o = B_{\nu,P_c}\tau_{\nu,P_c} - B_{\nu,(P_c-\Delta P)}\tau_{\nu,(P_c-\Delta P)} + \int_{\tau_{P_c}}^{\tau_{(P_c-\Delta P)}} B_\nu \, d\tau_\nu \quad \text{and} \tag{10}$$

$$\Delta R_\nu^u = B_{\nu,P_c}\tau_{\nu,P_c} - B_{\nu,(P_c+\Delta P)}\tau_{\nu,(P_c+\Delta P)} - \int_{\tau_{(P_c-\Delta P)}}^{\tau_{P_c}} B_\nu \, d\tau_\nu. \tag{11}$$

Figures 4 and 5 show ΔR_ν^o and ΔR_ν^u calculated for the standard and tropical atmosphere, respectively. For a cloud at 200 hPa (standard atmosphere), over- and underestimated radiance residuals are both very small; the MLEV can therefore be expected to perform less well under these conditions. It is particularly interesting to note that because of predominantly isothermal conditions at and above 200 hPa, underestimation of cloud pressure level results in a near-zero radiance residual ΔR_ν^u. For clouds at lower altitudes, both ΔR_ν^o and ΔR_ν^u values are considerably larger, with pronounced absorption line features of carbon dioxide and water vapor.

The corresponding modification to Eq. (4) results in expressions for the spectral effective emissivity $N\varepsilon_{c,\nu}$ derived from using overestimated ($N\varepsilon_{c,\nu,\text{over}}$) or underestimated ($N\varepsilon_{c,\nu,\text{under}}$) values for P_c:

$$N\varepsilon_{c,\nu,\text{over}} = \frac{R_\nu - R_{\text{clr},\nu}}{R_{\text{cld,over},\nu} - R_{\text{clr},\nu}} \quad \text{and} \tag{12}$$

$$N\varepsilon_{c,\nu,\text{under}} = \frac{R_\nu - R_{\text{clr},\nu}}{R_{\text{cld,under},\nu} - R_{\text{clr},\nu}}. \tag{13}$$

Figures 6 and 7 show $N\varepsilon_{c,\nu}$, $N\varepsilon_{c,\nu,\text{over}}$, and $N\varepsilon_{c,\nu,\text{under}}$ computed using Eqs. (4), (12), and (13) for four cloud-pressure-level cases (200, 300, 500, and 700 hPa), with a true $N\varepsilon_{c,\nu}$ of 1.0 under both standard and tropical atmosphere conditions. Each simulated radiance spectrum has a spectral resolution of 0.625 cm^{-1} and includes scene-dependent random Gaussian noise (i.e., scaled by the Planck function of the scene temperature; noise is assumed to be 0.25 K at 250-K scene temperature) to model that expected from the GIFTS instrument designed for the National Aeronautics and Space Administration (NASA) New Millennium Program (NMP; see section 3).

For the ideal case of $N\varepsilon_{c,\nu} = 1.0$ (i.e., opaque cloud), Figs. 6 and 7 demonstrate the unique characteristics of $N\varepsilon_{c,\nu,\text{over}}$ and $N\varepsilon_{c,\text{under}}$ [derived by assuming all variables in Eqs. (12) or (13) are known except for the cloud pressure level, which is either over- or underestimated] and the $N\varepsilon_{c,\nu}$ spectra [derived by assuming all variables in Eq. (4) are known perfectly]. High-frequency spectral variabilities of $N\varepsilon_{c,\nu,\text{over}}$ and $N\varepsilon_{c,\nu,\text{under}}$ are both higher

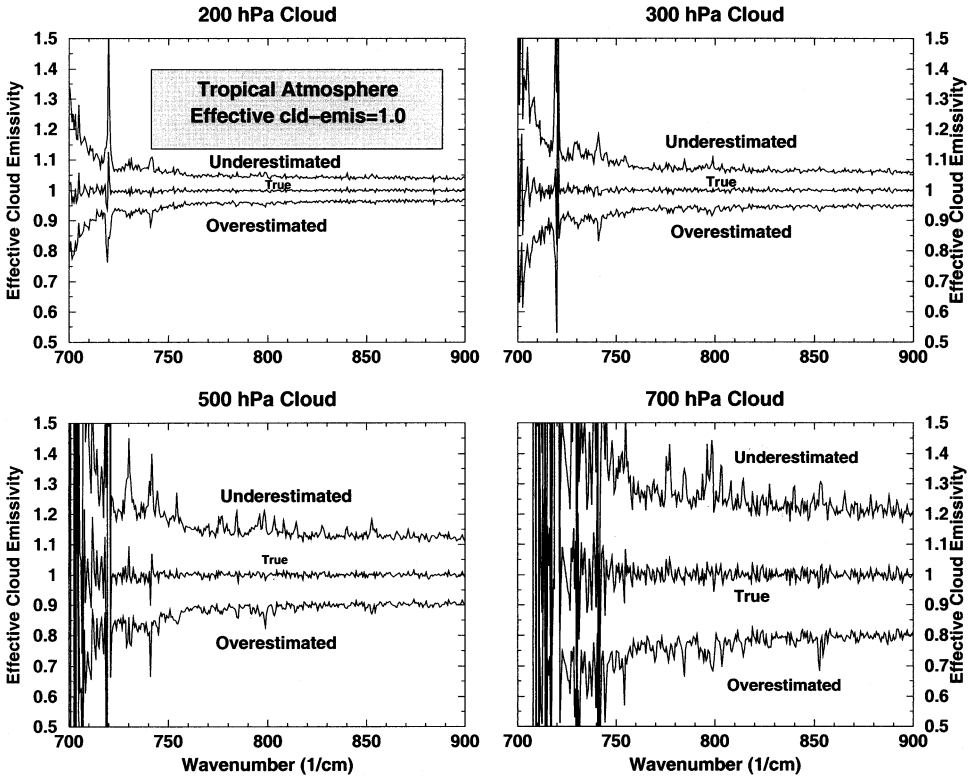

FIG. 7. Same as Fig. 6, but for tropical atmosphere.

than that of the true emissivity. This result is also true for other model atmospheres, such as midlatitude summer and midlatitude winter (not shown).

For semitransparent clouds ($N\varepsilon_{c,\nu} = 0.5$), similar radiance sensitivities to P_c and $N\varepsilon_{c,\nu}$ are also observed (not shown). That is, for both opaque and semitransparent (effective emissivity ~ 0.5) clouds, the optimal effective emissivity spectrum as depicted by the correct cloud pressure level exhibits the smallest local spectral variation for all levels of cloud under diverse atmospheric conditions. As was the case with cloud pressure level, the effective cloud emissivity information content able to be extracted by MLEV is greatest under a strong, monotonic lapse rate (tropical atmosphere) and warm conditions (summer case) for both opaque and semitransparent clouds.

Figures 8–10 show the local variances of effective cloud emissivity LEV(P_c), defined in Eq. (5), of overestimated, actual, and underestimated cloud levels at the true 200-, 500-, and 850-hPa cloud levels and under standard, tropical, midlatitude summer, and midlatitude winter atmosphere conditions. A constant spectral $N\varepsilon_{c,\nu}$ is used across channels for a range of $N\varepsilon_{c,\nu}$ values (0.2–1.0). For all cases, MLEVs are found and are associated with the correct cloud pressure level (labeled as ''true''). For the tropical atmosphere characterized by larger lapse rates and higher temperatures, MLEV clearly identifies the actual solution of the cloud parameters. For the 300-hPa case (not shown), MLEV generally performs well in retrieving the cloud pressure level, but its performance does decrease for the midlatitude-winter case. MLEV performance is at its peak for 500 hPa, or midlevel cloud (Fig. 9), even under near-transparent cloudy conditions ($N\varepsilon_{c,\nu} \sim 0.1$–$0.2$). For the 700-hPa level (not shown), MLEV performance once again decreases for the midlatitude-winter case, in which sensitivity is lost because of the cold and the reduced temperature lapse rate. Last, for the 850-hPa case (Fig. 10), near the top of the boundary layer, MLEV has less chance of being successful. Overestimation of cloud pressure level for warm cases and underestimation of cloud pressure altitude for cold cases are likely. The resulting cloud emissivity retrievals will therefore be less reliable at this level.

3. GIFTS simulation study results

In this section, a demonstration of MLEV retrieval of cloud pressure level and effective emissivity using simulated GIFTS longwave infrared measurements is presented. The design for the GIFTS instrument uses two detector arrays to cover the spectral bands 685–1150 cm^{-1} (longwave) and 1650–2250 cm^{-1} (short-/medium wave) at a spectral resolution of 0.625 cm^{-1}. A set of 177 profiles covering the region between 10° and 35°N latitude and between 90° and 110°W longitude

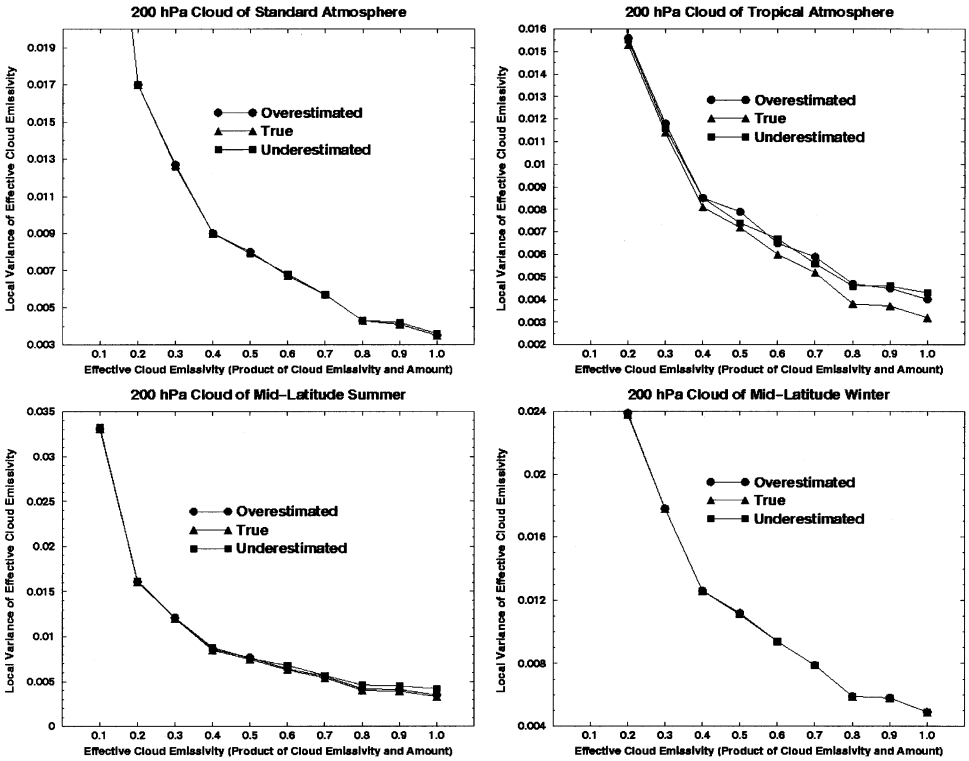

FIG. 8. Local variance of effective cloud emissivity derived from overestimated (cloud at 150 hPa), true (cloud at 200 hPa), and underestimated (cloud at 250 hPa) cloud level for four different atmosphere conditions: standard, tropical, midlatitude summer, and midlatitude winter.

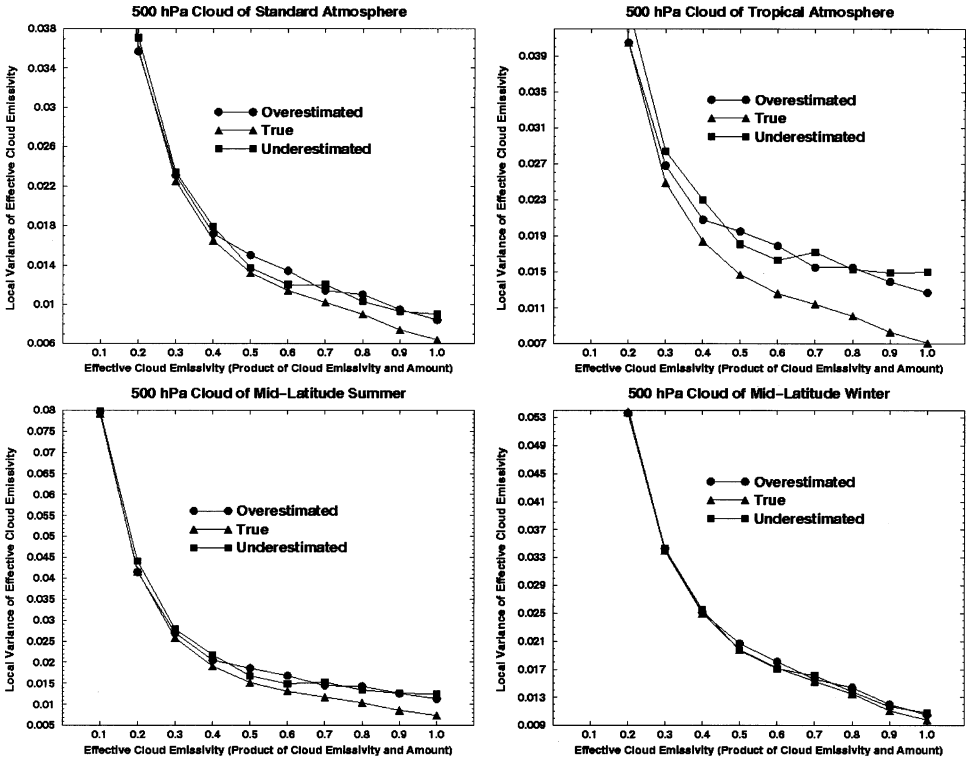

FIG. 9. The same as Fig. 8, except clouds are located at 450 (overestimated), 500 (true), and 550 (underestimated) hPa.

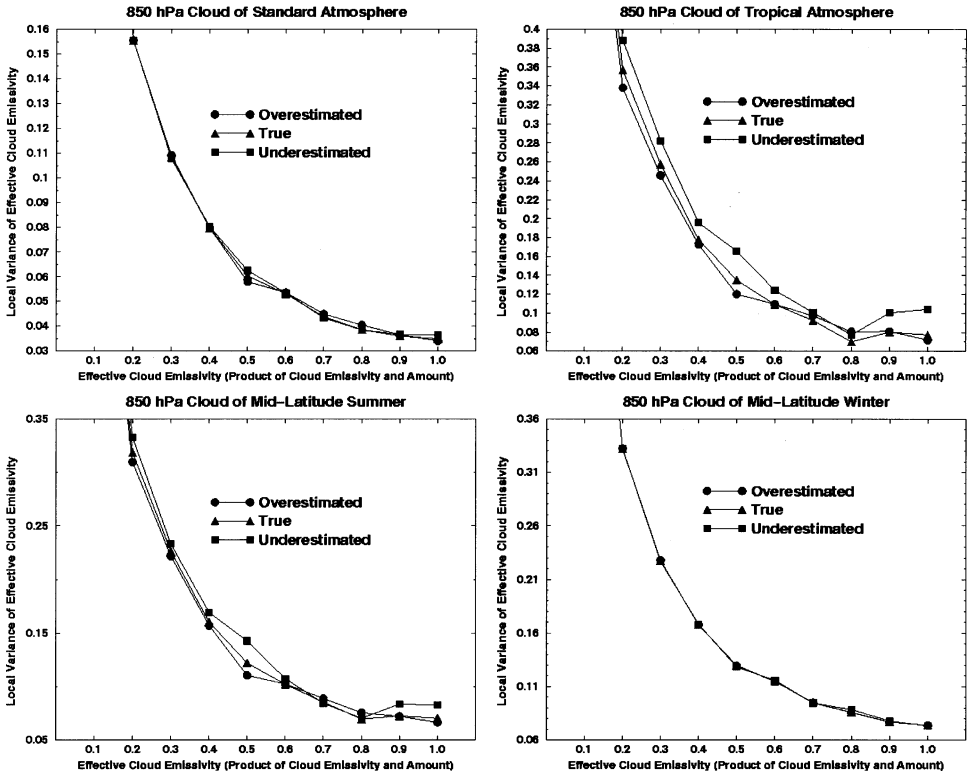

FIG. 10. The same as Fig. 8, except clouds are located at 800 (overestimated), 850 (true), and 900 (underestimated) hPa.

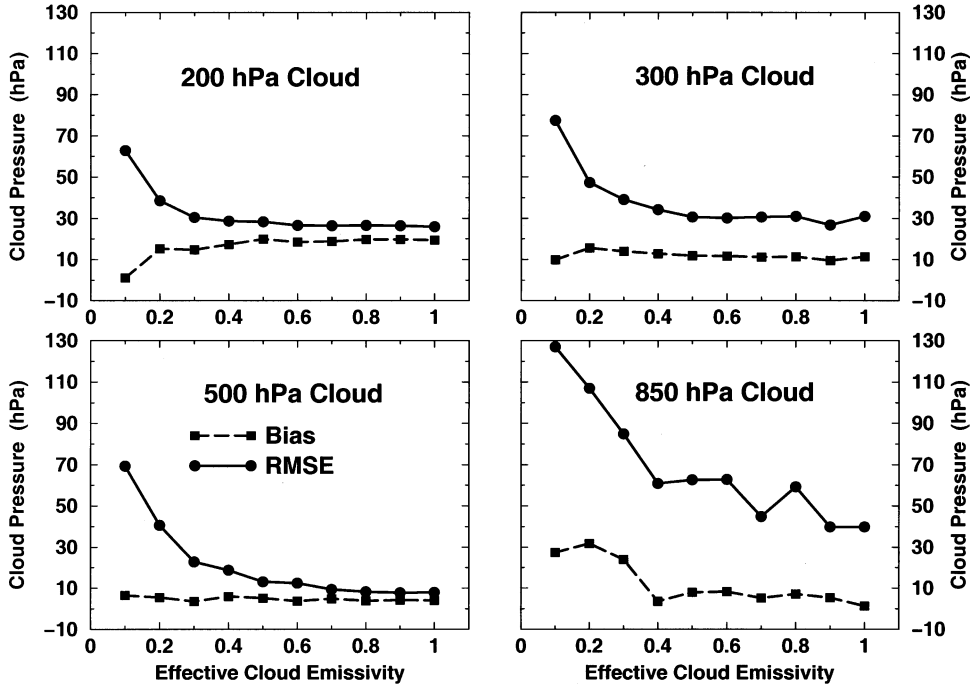

FIG. 11. MLEV cloud pressure level bias and rmse vs effective cloud emissivity for four different cloud levels.

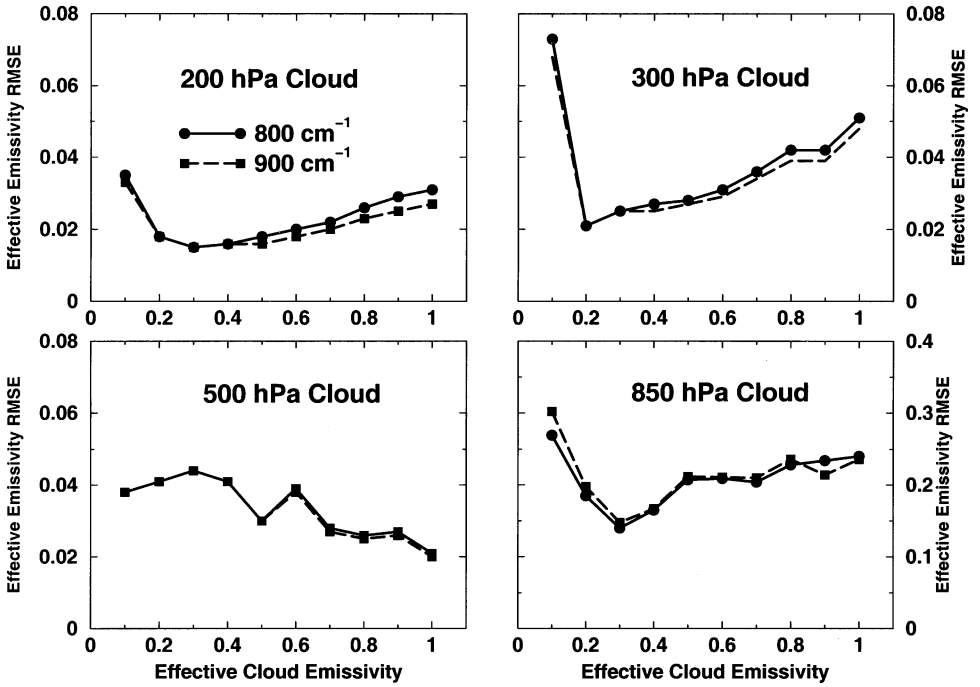

FIG. 12. Effective cloud emissivity rmse for 800 and 900 cm^{-1} vs effective cloud emissivity for four different cloud levels.

throughout 2000, representing a diverse set of atmospheric conditions within part of the planned GIFTS geographical coverage, was selected for this demonstration. Forty combinations were formed from each profile by assigning four cloud heights (200, 300, 500, and 850 hPa representing very high, high-, medium-, and low-level clouds) and 10 effective emissivities [0.1, 0.2, . . . , 0.9, and 1.0, corresponding to low cloud cover (or transparent clouds) through overcast (or opaque cloudy conditions)]. The GIFTS longwave cloudy ra-

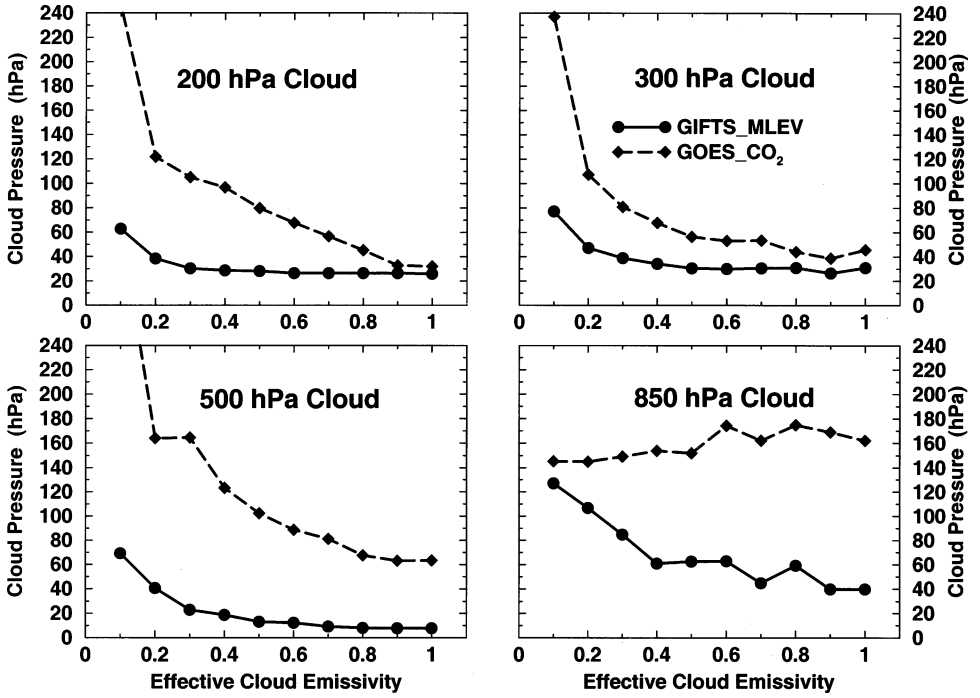

FIG. 13. A comparison of simulated GIFTS MLEV-retrieved cloud pressure level rmse and GOES results.

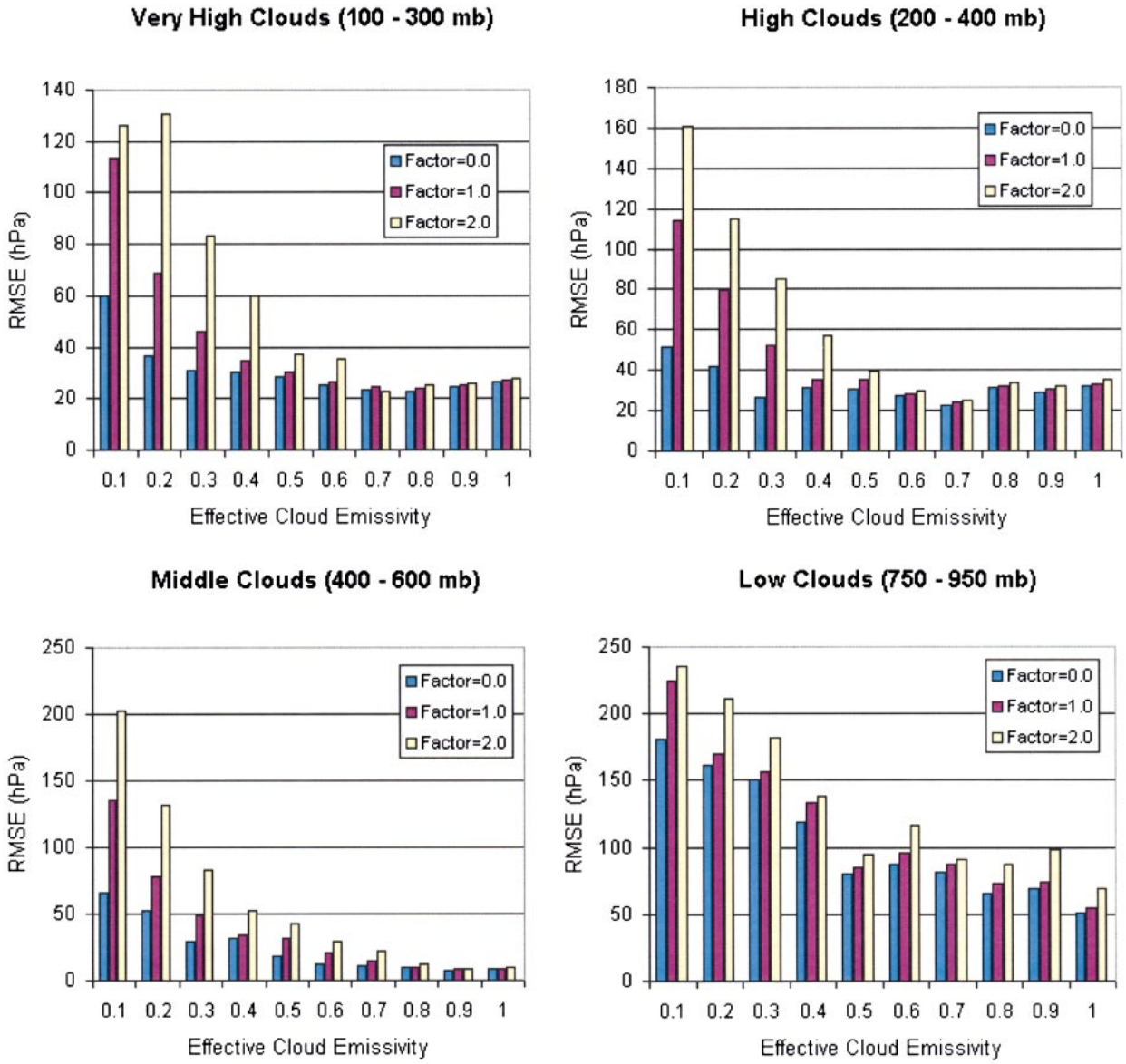

FIG. 14. MLEV cloud pressure rmse for four cloud pressure level ranges as the function of clear radiance errors. The clear radiance observation errors are assumed to be no error (factor = 0), nominal (factor = 1), and 2 times nominal (factor = 2).

diance spectra, using Eq. (3), were simulated for all 40 combinations of each profile. No spectral emissivity variation was introduced, and a simulated GIFTS baseline measurement random noise of 0.25 K at 250 K was added. Figure 11 displays MLEV cloud pressure level root-mean-square error (rmse) and bias as functions of cloud pressure levels (four panels) and effective cloud emissivity (horizontal axis). Rmse and bias are computed from the differences of MLEV-retrieved and simulated true cloud pressure and emissivity for all cases classified as a function of four cloud pressure levels and 10 effective cloud emissivities. Rmse and bias can be explained as the statistical error bars for MLEV performance in terms of retrieval standard deviation and systematic error.

The results indicate that the MLEV algorithm shows little bias for all levels of clouds and opaqueness. Except for transparent clouds (i.e., $N\varepsilon_{c,\nu} < 0.2$), retrieval rmse of cloud pressure level is approximately 30 hPa for high and very high clouds and is approximately 10 hPa for midlevel clouds. For low clouds, rmse increases to approximately 50 hPa and a large error becomes apparent for transparent clouds. Figure 12 is similar to Fig. 11, except for the MLEV-derived cloud emissivity rmse for 800 and 900 cm^{-1}. Again, the four panels represent four different levels of simulated clouds; effective emissivity

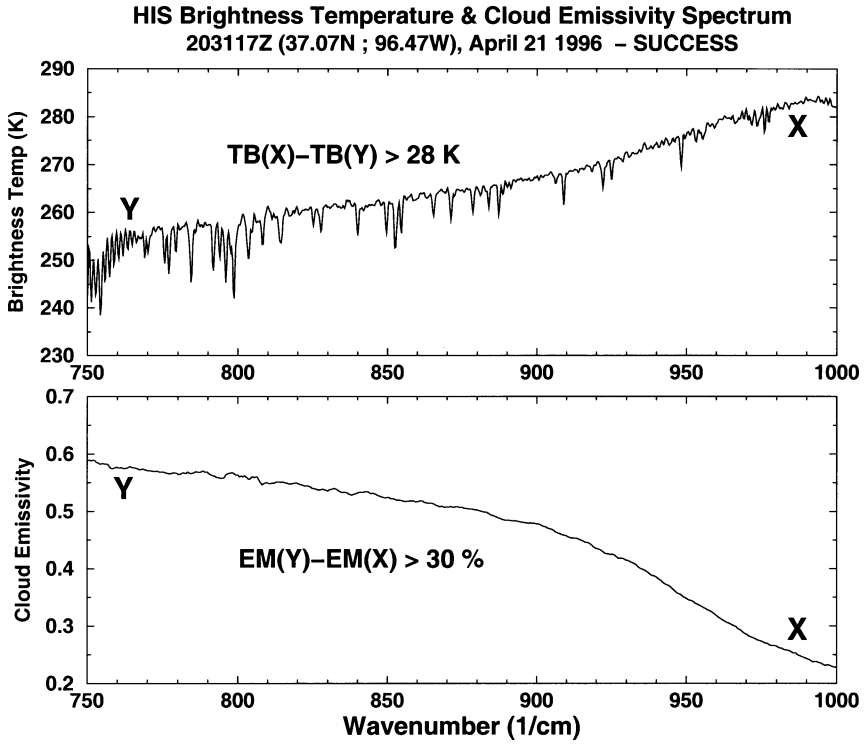

FIG. 15. Example (top) cloud brightness temperature and (bottom) MLEV effective emissivity spectra of HIS on 21 Apr 1996. Large spectral variation is an indication of very small particle ice crystals of contrails.

rmse for both wavenumbers are also shown as a function of effective cloud emissivity. For medium- and higher-level clouds, the average rmse of $N\varepsilon_{c,\nu}$ varies from about 0.02 to 0.05, except for very transparent cloud. For the low-cloud case, significant degradation in performance of MLEV $N\varepsilon_{c,\nu}$ can be seen. At this cloud level, the retrieved effective emissivity rmse is approximately 0.2. For comparison, CO_2-slicing cloud pressure level retrieval using Geostationary Operational Environmental Satellite (GOES) sounder data (Menzel and Purdom 1994) and GIFTS MLEV retrieval cloud pressure level rmse is presented in Fig. 13. The cloud pressure level information content of GOES and simulated GIFTS data demonstrates the potential improvement of high-spectral-resolution measurements over filter radiometer measurements.

The results shown in Figs. 11–13 all assume atmospheric uncertainties of 1.0 K for the temperature profile, 1.0 K for surface skin temperature, and 15% for water vapor profile to calculate clear and cloudy radiances. To assess further the impact of the uncertainty of clear radiances on MLEV performance, Fig. 14 demonstrates the MLEV cloud pressure rmse for four cloud pressure level ranges (100–300, 200–400, 400–600, and 750–950 hPa) that represent clouds from very high to low-altitude cases for three different clear radiance errors. The clear radiance observation errors are assumed to be no error (factor = 0), nominal (factor = 1), and 2 times nominal (factor = 2), where nominal error is defined as the standard channel-dependent measurement error.

In summary, the uncertainty of clear radiances can lead to significant degradation of MLEV cloud pressure estimates when effective cloud amount is less than 0.4. For relatively opaque clouds (effective cloud amount greater than 0.4), nominal and 2-times-nominal clear radiance errors have small impacts on the cloud pressure retrieval for all levels of clouds, except for low clouds (750–950 hPa).

4. HIS MLEV SUCCESS field experiment results

The SUCCESS field experiment, conducted from 8 April to 10 May 1996, was cosponsored by NASA's Subsonic Assessment Program and Radiation Sciences Program. A number of NASA aircraft were used in the campaign, including a medium-altitude DC-8, which carried a wide variety of gaseous, particulate, radiative, and meteorological instruments and was used primarily as an in situ sampling platform, and a high-altitude ER-2, which was acting as a surrogate satellite and carried the HIS (along with other instruments) so that remote sensing observations could be related to the in situ measurements of the DC-8.

HIS data acquired from the ER-2 on 21 April 1996 were selected for the demonstration of MLEV cloud

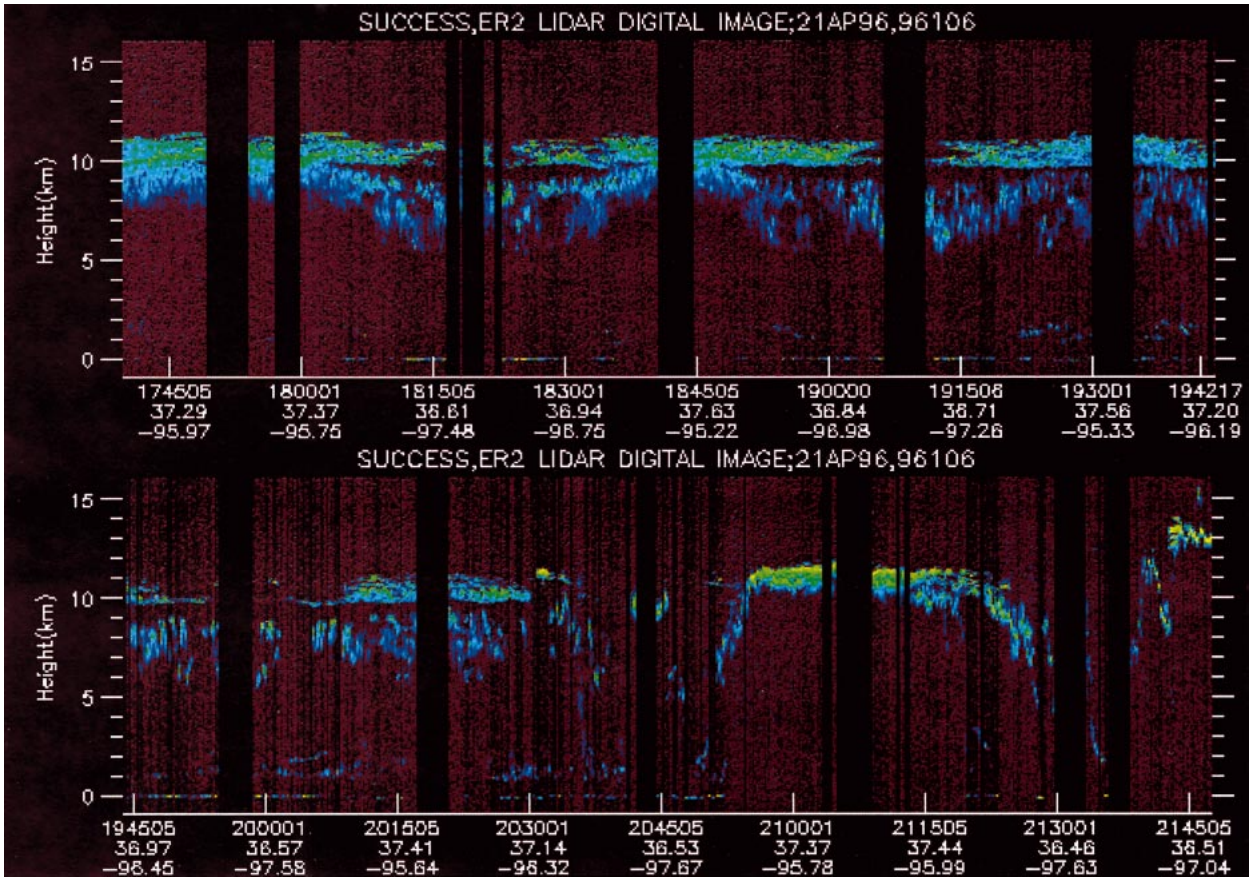

FIG. 16. Time series of CLS return signal cross section. Bright green and blue indicate cloud vertical structure.

spectral emissivity retrieval. The HIS observed the spectral radiance of a 4–5-min-old contrail that had been created by the DC-8 flying below at a pressure level of 250 hPa. Inspection of coincident Moderate-Resolution Imaging Spectroradiometer (MODIS) Airborne Simulator (MAS; King et al. 1996) imagery showed that the contrail was relatively diffuse by the time the ER-2 passed over it. The brightness temperature of the cirrus across the 10–12-μm window varied over 28 K (Fig. 15, upper panel), corresponding to a variation in the MLEV-derived emissivity of 30% (Fig. 15, lower panel). The spectral character of this large variation of optical depth is a signature of very small ice crystals.

Validation data for these results were provided by the cloud lidar system (CLS; Spinhirne and Hart 1990) contained within the left ER-2 superpod. A CLS cross-sectional backscatter signal image over the period from 1745 to 2145 UTC 21 April is shown in Fig. 16. The processed data that identified only the single-layer cloud below the ER-2 were then used to validate the MLEV-derived cloud pressure level and emissivity spectrum.

Figure 17 illustrates the fundamental principle of the MLEV by showing five emissivity spectra generated from HIS data during the MLEV process, corresponding to five ''first guess'' pressure levels. The middle curve, corresponding to the 300-hPa pressure level, exhibits the minimum spectral variance (rms = 1%). As we have seen, the cloud pressure associated with the emissivity spectrum showing the minimum spectral variance is the algorithm's best-estimate output. In this case, the derived cloud pressure level is in good agreement with that of 280 hPa determined by the CLS. Figure 18 shows a time series of the retrieval cloud level derived from both the CLS and MLEV algorithm, as well as the MLEV-derived cloud emissivity at a wavenumber of 900 cm^{-1}. At approximately record 210 (2112 UTC), when the cloud emissivity is near 0.2, MLEV overestimated the cloud height. For all other time periods, the MLEV performed consistently with CLS measurements, for varying emissivities from opaque (emissivity = 1) to semitransparent (emissivity = 0.2). The relatively good performance of the single-layer SUCCESS cloud pressure is indicative of high sensitivity of MLEV for high- (200–300 hPa) and opaque- (mean emissivity of ~0.75) cloud cases. The calculated mean cloud pressure error is about 18 hPa for cloud around 200–300 hPa. For lower-cloud cases (below 500 hPa), mean cloud pressure error is about 20–70 hPa. The higher errors are also due to the relatively low cloud emissivity (~0.2–0.4).

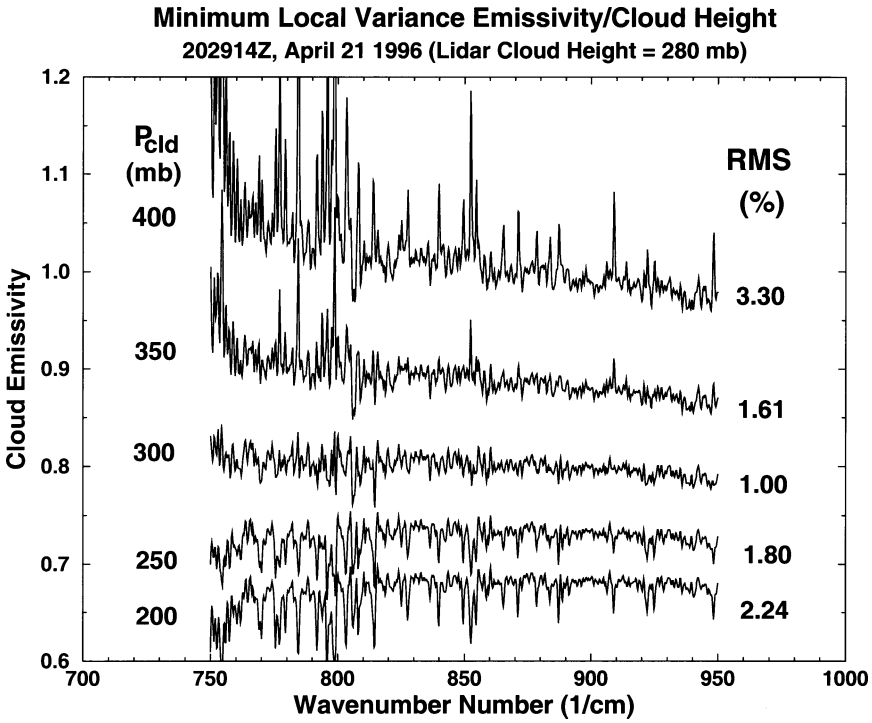

FIG. 17. Example of MLEV. For optimal retrieval cloud altitude (300 hPa), local emissivity variance is minimum (1%). True cloud altitude is measured by CLS as 280 hPa.

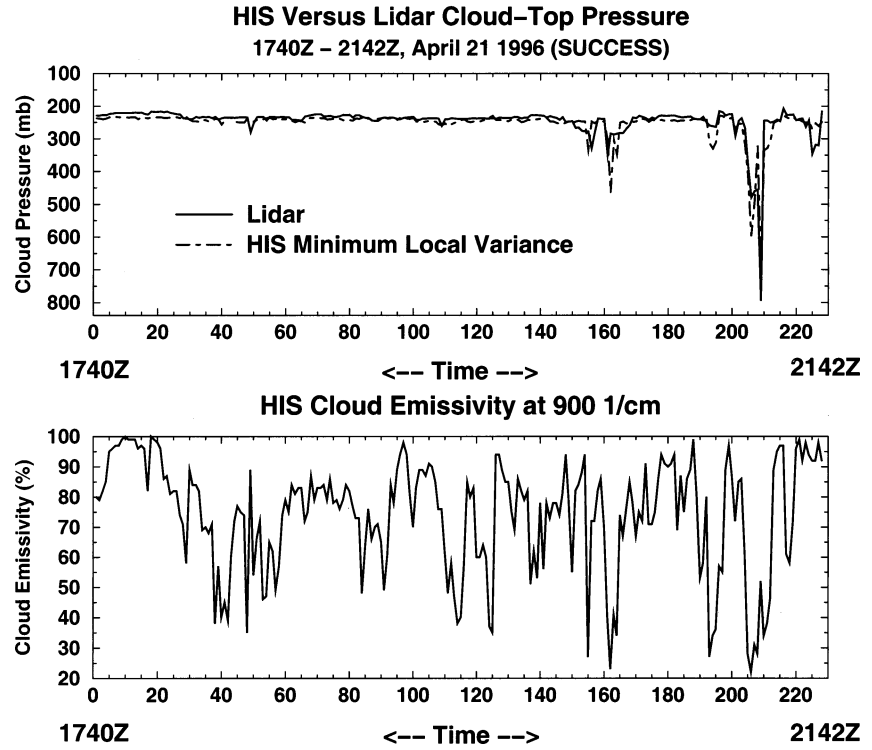

FIG. 18. Time series of (top) MLEV cloud altitude and (bottom) effective emissivity at 900 cm^{-1} for 21 Apr 1996 HIS measurements. Single-layer cirrus cloud altitude determined by CLS is also overlaid for verification.

5. Discussion and conclusions

MLEV is a relatively simple single-layer cloud technique that takes advantage of the high spectral resolution of cloud-sensitive longwave infrared radiance measurements that is possible with new instruments to determine cloud pressure level and the effective spectral emissivity simultaneously. The optimal cloud pressure level and emissivity spectrum solution derived from MLEV is that which yields the smallest local spectral variation of the derived emissivity spectrum.

Because a cloud absorbs, reflects, scatters, and radiates smoothly within a localized spectral region, any abrupt high-frequency feature existing in the retrieved emissivity spectrum is indicative of suboptimal cloud pressure level determination, which is the dominant factor in obtaining the cloud emissivity spectrum retrieval.

In this simulation study, it is shown that the MLEV cloud pressure root-mean-square errors for a single-layer cloud with effective cloud emissivity greater than 0.1 are ~30, ~10, and ~50 hPa for high (200–300 hPa), middle (500 hPa), and low (850 hPa) clouds, respectively. The associated cloud emissivity root-mean-square errors in the 900 cm^{-1} spectral channel are less than 0.05, 0.04, and 0.25 for high, middle, and low clouds, respectively. Only a single real observation example of MLEV retrieval has been given in this paper; additional investigations of MLEV performance are planned by the authors that will make use of the National Polar-Orbiting Environmental Satellite System (NPOESS) Airborne Sounder Testbed—Interferometer (NAST-I; Smith et al. 2001) and Scanning HIS (S-HIS; Revercomb et al. 1996) high-altitude aircraft data together with measurements from the collocated cloud lidar. Further efforts will also be directed toward the application of MLEV-derived emissivity spectra to forward modeling, that is, creating simulated radiances of cloudy fields of view for use in other radiative transfer and remote sensing studies. In addition, extension of MLEV to the multiple-cloud-layer case and retrieval of cloud microphysical properties such as cloud particle size and cloud optical thickness are other promising applications of MLEV that deserve further study.

Acknowledgments. This research was partially supported by NASA NMP Contract NAS1-00072, NOAA Grant NA07EC0676, and U.S. Navy MURI Research Grant N00014-01-0850.

REFERENCES

Eyre, J. R., and W. P. Menzel, 1989: Retrieval of cloud parameters from satellite sounder data: A simulation study. *J. Appl. Meteor.*, **28,** 267–275.

Huang, B., W. L. Smith, H.-L. Huang, and H. M. Woolf, 2002: Comparison of linear forms of the radiative transfer equation with analytic Jacobians. *Appl. Opt.*, **41,** 4209–4219.

Huang, H.-L., and Coauthors, 2000: Geostationary Imaging FTS (GIFTS) data processing: Measurement simulation and compression. *Proc. SPIE,* **4151,** 103–114.

King, M. D., and Coauthors, 1996: Airborne scanning spectrometer for remote sensing of cloud, aerosol, water vapor, and surface properties. *J. Atmos. Oceanic Technol.,* **13,** 777–794.

Li, J., W. P. Menzel, and A. J. Schreiner, 2001: Variation retrieval of cloud parameters from GOES sounder longwave cloudy radiance measurements. *J. Appl. Meteor.*, **40,** 312–330.

Menzel, W. P., and J. F. W. Purdom, 1994: Introducing GOES-I: The first of a new generation of Geostationary Operational Environmental Satellites. *Bull. Amer. Meteor. Soc.,* **75,** 757–781.

——, W. L. Smith, and T. R. Stewart, 1983: Improved cloud motion wind vector and altitude assignment using VAS. *J. Climate Appl. Meteor.*, **22,** 377–384.

Revercomb, H. E., and Coauthors, 1996: Airborne and ground-based Fourier transform spectrometers for meteorology: HIS, AERI and the new AERI-UAV. *Optical Instruments for Weather Forecasting,* G. W. Kamerman, Ed., International Society for Optical Engineering (SPIE Vol. 2832), 106–117.

Smith, W. L., and C. M. R. Platt, 1978: Intercomparison of radiosonde, ground-based laser, and satellite-deduced cloud heights. *J. Appl. Meteor.*, **17,** 1796–1802.

——, H. E. Revercomb, H.-L. Huang, and R. O. Knuteson, 1993: Vertical sounding capabilities with high spectral resolution atmospheric radiation measurements—A demonstration with the High Resolution Interferometer Sounder (HIS). *High Spectral Resolution Infrared Remote Sensing for Earth's Weather and Climate Studies,* A. Chedin, M. T. Chahine, and N. A. Scott, Eds., Springer-Verlag, 131–146.

——, D. K. Zhou, F. W. Harrison, H. E. Revercomb, A. M. Larar, H.-L. Huang, and B. Huang, 2001: Hyperspectral remote sensing of atmospheric profiles from satellite and aircraft. *Proc. SPIE,* **4151,** 94–102.

Spinhirne, J. D., and W. D. Hart, 1990: Cirrus structure and radiative parameters from airborne lidar and spectral radiometer observations: The 28 October 1986 FIRE study. *Mon. Wea. Rev.*, **118,** 2329–2343.

Toon, O. B., and R. C. Miake-Lye, 1998: Subsonic Aircraft: Contrail and Cloud Effects Special Study (SUCCESS). *Geophys. Res. Lett.,* **25,** 1109–1112.